EEET ECOLOGICAL ENGINEERING & ENVIRONMENTAL TECHNOLOGY

*Ecological Engineering & Environmental Technology*, 2026, 27(6), 227–235
https://doi.org/10.12912/27197050/221309
ISSN 2719–7050, License CC-BY 4.0

Received: 2026.04.17
Accepted: 2026.05.18
Published: 2026.06.01

# Development of carbon monoxide based materials from oyster and clam shells for metal ion removal from aqueous media and proposal of the underlying mechanism

Trung Minh Dao[1*], Nha Thanh Tran[2], Trung Xuan Nguyen[2], Bao Thai Pham Le[2], An The Huynh[2]

[1] Institute for Environmental Science, Engineering and Management, Industrial University of Ho Chi Minh City, Ho Chi Minh City, Vietnam
[2] Institute of Green and Sustainable Technology, Thu Dau Mot University, Ho Chi Minh City, Vietnam
* Corresponding author's e-mail: daominhtrung@iuh.edu.vn

## ABSTRACT

This study evaluates the potential of calcined oyster and clam shells as low-cost materials for the removal of heavy metal ions $Pb^{2+}$, $Cd^{2+}$, and $Cu^{2+}$ in aqueous solutions. The materials were collected, cleaned, and calcined at 700 °C to produce carbon monoxide (CaO)-rich materials. Material characterization was performed using Fourier-transform infrared spectroscopy (FTIR), scanning electron microscopy (SEM,) and Brunauer-Emmett-Teller analysis (BET). The FTIR results confirmed the partial conversion of $CaCO_3$ to CaO, while SEM images showed a strongly aggregated particle structure and dense surface. BET analysis revealed very low specific surface areas (1.049 and 0.373 $m^2/g$ for oyster and clam shells, respectively), indicating poorly developed capillary structures. Despite this, both materials achieved high removal efficiency, particularly for $Pb^{2+}$(>90% at a concentration of 150 mg/L). The treatment efficiency followed the order $Pb^{2+} > Cd^{2+} > Cu^{2+}$, consistent with the physicochemical properties and precipitation capabilities of the metal ions. The results showed that the removal mechanism was not dominated by physical adsorption but mainly involved chemical processes, including CaO hydration to create an alkaline environment, precipitation of hydroxides and carbonates, and ion exchange. The study demonstrated that calcined seashell material is an effective, sustainable, and low-cost solution for heavy metal treatment in water.

**Keywords:** calcined shell waste, oyster shells, clam shells, heavy metal removal, chemical precipitation, CaO-based materials, ion exchange, wastewater treatment.

## INTRODUCTION

The rapid increase in industrial production activities, from mineral extraction and electroplating to battery and chemical manufacturing, has led to a serious accumulation of heavy metal ions in aquatic environments (Oladimeji et al., 2024). Unlike biodegradable organic pollutants, heavy metals such as lead, cadmium, and copper are persistent, highly toxic, and accumulate along the food chain, causing unpredictable consequences for human health, such as kidney failure, central nervous system damage, and cancer (Ali et al., 2019, Balali-Mood et al., 2021). In countries with long coastlines and a thriving aquaculture industry like Vietnam, finding a wastewater treatment solution that is both effective and utilizes local by-products is becoming a pressing challenge in sustainable development strategies. Among current wastewater treatment techniques, adsorption is the preferred method due to its high efficiency, simple operation process, and reusability of materials (Rashid et al., 2021). However, the biggest barrier to large-scale application is the cost of producing commercially available adsorbent materials. This has driven a trend of researching the use of biomaterials derived from abundant natural sources. Oyster shells and clam shells, which are often considered environmentally polluting waste, could be seen as potential raw materials.

Recent studies have confirmed that oyster shells are a versatile bioadsorbent material capable of effectively treating various heavy metals through different processing methods. Specifically, oyster shells can be used in their original form to treat rainwater with a removal efficiency of 80–95% for $Cu^{2+}$ and 50–90% for $Cd^{2+}$ (Xu et al., 2021). When ground into powder, this material follows a second-order kinetic model, in which the adsorption of $Cu^{2+}$ and $Cd^{2+}$ conforms to the Langmuir isotherm, while $Pb^{2+}$ conforms to the Freundlich isotherm, with preferential removal in the order $Pb^{2+} > Cd^{2+} > Cu^{2+}$ (Xu et al., 2019). At a more advanced processing level, oyster shells calcined at 800 $^0$C will completely transform into CaO with a mesoporous structure, creating coordination centers and hydroxyl functional groups that effectively remove $Ni^{2+}$, $Zn^{2+}$ and $Mn^{2+}$ through complex formation in an alkaline environment (Xia et al., 2021). Furthermore, recycling oyster shells into vaterite-type $CaCO_3$ microparticles showed particularly impressive $Pb^{2+}$ removal efficiency (99.9%) due to ion exchange reactions between $Ca^{2+}$ and heavy metals leading to recrystallization (Lin et al., 2020). These results show that utilizing oyster shell waste not only helps minimize solid waste pollution but also provides a low-cost, high-efficiency solution for water filtration systems from household to urban infrastructure (Lin et al., 2020; Xia et al., 2021; Xu et al., 2021).

Similar to oyster shells, clam shells also show great potential when transformed into advanced adsorbent materials through chemical modification methods. One effective approach is the synthesis of hydroxyapatite from clam shell waste by wet precipitation. This material achieved impressive adsorption capacities at pH 5 with values of 265, 64, and 55 mg/g for $Pb^{2+}$, $Cd^{2+}$, and $Cu^{2+}$, respectively (Núñez et al., 2019). Furthermore, clam shells can be magnetized in combination with calcination to create materials such as CECS or CCCS, achieving a maximum adsorption capacity of up to 266.5 mg/g of $Cd^{2+}$, with precipitation and cation exchange mechanisms playing a dominant role (accounting for > 60%) (Wang et al., 2024). In addition, surface modification with citric acid breaks down the original structure to expose more carboxyl groups and a larger surface area, thereby increasing the adsorption efficiency of $Pb^{2+}$ by approximately 35–62% compared to raw clam shells (Sun et al., 2016). These studies agree that the adsorption process on modified clam shells generally follows second-order kinetics and the Langmuir isotherm model, and confirm the high reusability and wide application prospects from wastewater treatment to the remediation of soil contaminated with heavy metals (Sun et al., 2016, Wang, et al., 2024). Based on previous studies, this research evaluates the ability of heat-treated clam and oyster shell materials in Vietnam to remove $Pb^{2+}$, $Cd^{2+}$, and $Cu^{2+}$ ions from water.

## EXPERIMENTAL

### Preparation of calcined oyster shells, clam shells

Oyster and clam shells were collected from a food restaurant in Ho Chi Minh City, Vietnam. Afer collection, these shells were soaked and washed several times with water, then soaked overnight in NaOH 0.1 M solution to remove dissolved impurities on the surface. They were then rinsed again with distilled water until the pH of the washing solution remained constant. Afterwards, the oyster and clam shells were dried at 120 °C for 24 hours, ground, and sieved to obtain particles with a size < 1 mm. The entire powder sample was then calcined at 700 °C for 2 hours to obtaine material (Rosli et al., 2024).

### Metal ion removal process and calculation methods

The removal of heavy metal ions ($Pb^{2+}$, $Cd^{2+}$, and $Cu^{2+}$) from aqueous solutions was conducted using a batch experimental method. Stock solutions of $Pb(NO_3)_2$, $Cd(NO_3)_2{\cdot}4H_2O$, and $Cu(NO_3)_2{\cdot}3H_2O$ were prepared using analytical-grade reagents and deionized water. Working solutions with initial concentrations of 50, 100, and 150 mg/L were obtained by appropriate dilution.

For each experiment, 0.5 g of calcined oyster shell or calcined clam shell material was accurately weighed and placed into a 50 mL Erlenmeyer flask. Subsequently, 30 mL of metal ion solution was added. The mixtures were agitated in a mechanical shaker at a constant speed of 120 rpm for 90 minutes at room temperature (25 ± 2 °C).

The initial pH of the solutions was not adjusted in order to investigate the intrinsic alkalinity generated by the calcined materials. After the reaction, the suspensions were filtered through Whatman filter paper to separate the solid phase. The filtrates were collected for further analysis.

The concentrations of $Pb^{2+}$, $Cd^{2+}$, and $Cu^{2+}$ before and after treatment were determined using inductively coupled plasma mass spectrometry (ICP-MS). All experiments were performed in triplicate, and the average values were reported.

The adsorption capacity (Qe, mg/g), defined as the amount of metal ions removed per unit mass of adsorbent, was calculated as follows:

$$q_e = \frac{(C_0 - C_e).\ V}{m} \quad (1)$$

where: $q_e$ (mg/g) is the adsorption capacity at equilibrium, $C_0$ (mg/L) is the initial concentration, $C_e$ (mg/L) is the equilibrium concentration after treatment, $V$ (L) is the solution volume, and $m$ (g) is the mass of the adsorbent.

The removal efficiency (H, %) was determined using the following equation:

$$H = \frac{C_0 - C_e}{C_0} \times 100 \quad (2)$$

where: $H$ (%) represents the removal efficiency, $C_0$ (mg/L) is the initial concentration, and $C_e$ (mg/L) is the concentration after treatment.

### Material characterizations

The FTIR spectra were recorded using a Nicolet Nexus 670 FTIR Spectrometer. The SEM images were obtained using a Hitachi S-4800 Microscope. The BET result was taken by NOVA 4000e of Quantachrome.

### Data processing and statistical analysis

All experimental data were processed and analyzed using Microsoft Excel and Statgraphics software. Microsoft Excel was used for preliminary data handling, including calculation of removal efficiency (H, %) and adsorption capacity (Qe, mg/g), as well as data organization and graphical representation.

Statistical analysis was performed using Statgraphics Centurion software to evaluate the reliability and significance of the experimental results. All experiments were conducted in triplicate, and the results are presented as mean values ± standard deviation (SD).

Analysis of variance (ANOVA) was applied to assess the statistical significance of differences between experimental conditions, with a confidence level of 95% ($p < 0.05$). In addition, regression analysis was used to examine the relationship between initial metal ion concentration and removal performance.

These statistical methods ensured the accuracy, reproducibility, and reliability of the experimental data.

## RESULTS AND DISCUSSION

### Characterization of calcined oyster shells, clam shells

The FTIR spectra of two sample inluding calcined oyster shells and calcined clam shells displayed the same tendency (Figure 1). Both spectra exhibited characteristic absorption bands of carbonate ions ($CO_3^{2-}$), with a strong peak observed in 1415 and 1422 $cm^{-1}$, respectively, which is attributed to the asymmetric stretching vibration ($\nu_3$) of the $CO_3^{2-}$ group. Additionally, a distinct band at approximately around 870–880 $cm^{-1}$ corresponds to the out-of-plane bending vibration ($\nu_2$) of carbonate, further confirming the presence of $CaCO_3$ in the original material. However, the intensity of the absorption band related to $CO_3^{2-}$ group is not well in both samles, indicating thermal decomposition of $CaCO_3$ to form CaO and $CO_2$ release. The appearance of absorption bands in the around 500–600 $cm^{-1}$ region, characteristic of the stretching vibrations of the Ca-O bond, provides direct evidence for the formation of the calcium oxide phase. Notably, no absorption bands were observed at around 3400 $cm^{-1}$ and 1600 $cm^{-1}$, suggesting that the calcined material does not contain significant amounts of adsorbed hydroxyl groups or water, indicating that the material surface is relatively anhydrous and has not been hydrated to $Ca(OH)_2$. For both samples, the FTIR results confirm the partial decomposition of $CaCO_3$ into CaO. Based on the current spectra, a definitive comparison of the conversion degree between the oyster and clam shells cannot be conclusively established.

The SEM images of the two oyster and clam shell samples after calcination show a marked change in surface morphology (Figure 2 and 3). Both samples exhibit heterogeneous particles with sizes distributed in the micro-submicrometer range, and a strong tendency to aggregate into large clusters. This phenomenon

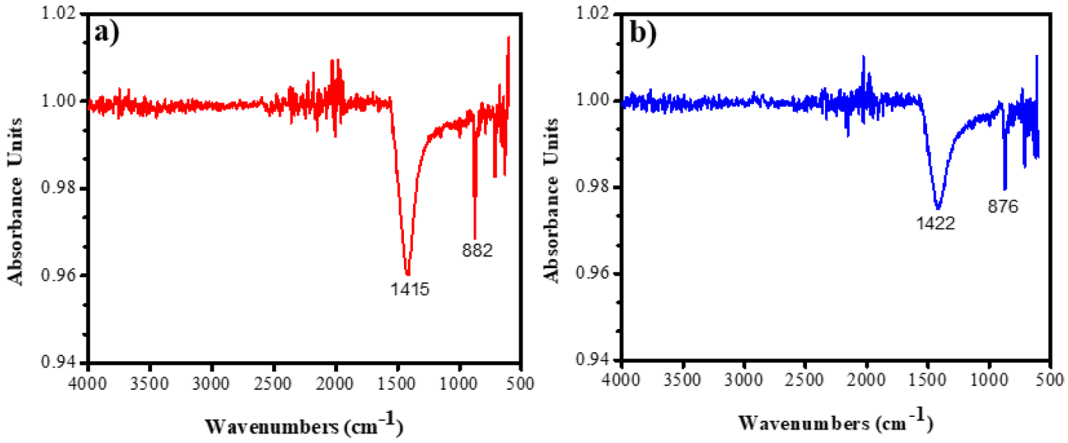


**Figure 1.** The FTIR spectrum of calcined oyster shells, clam shells

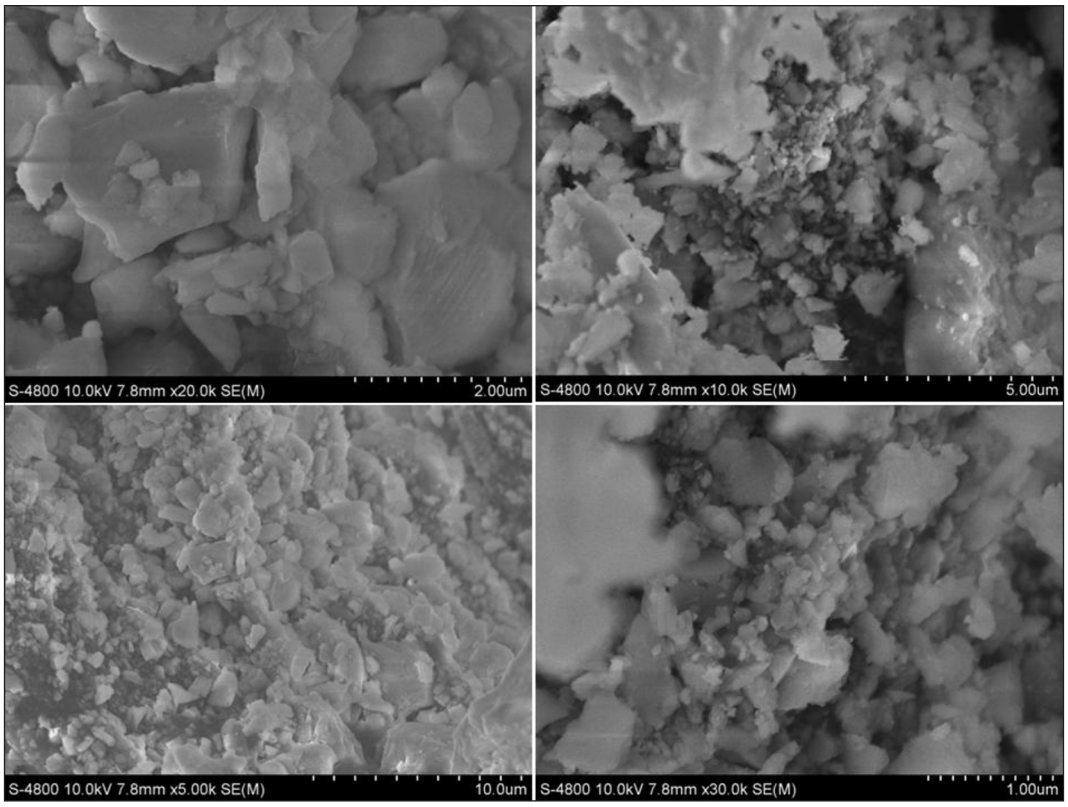


**Figure 2.** The scanning electon microscopy images of calcined oyster shells

suggests that the calcination process disrupted the characteristic layered structure of $CaCO_3$ in the biological shell, while promoting adhesion and rearrangement of material particles, related to sintering and the formation of the CaO phase after thermal decomposition. At high magnifications, the surfaces of both samples show a rather dense structure with tightly bound particles, and indistinct particle boundaries in many areas, especially in the oyster shell sample. This reflects strong agglomeration and coalescence, leading to a reduction in effective surface area. Although some small gaps and microcracks between the particles were observed, possibly formed by the release of $CO_2$ gas during the decomposition of $CaCO_3$, these voids were scattered and did not form a continuous pore system.

This suggests inefficient pore formation and possible pore collapse during high-temperature calcination. Qualitative comparison between the two samples revealed that the oyster shell sample tended to form larger particle clusters and

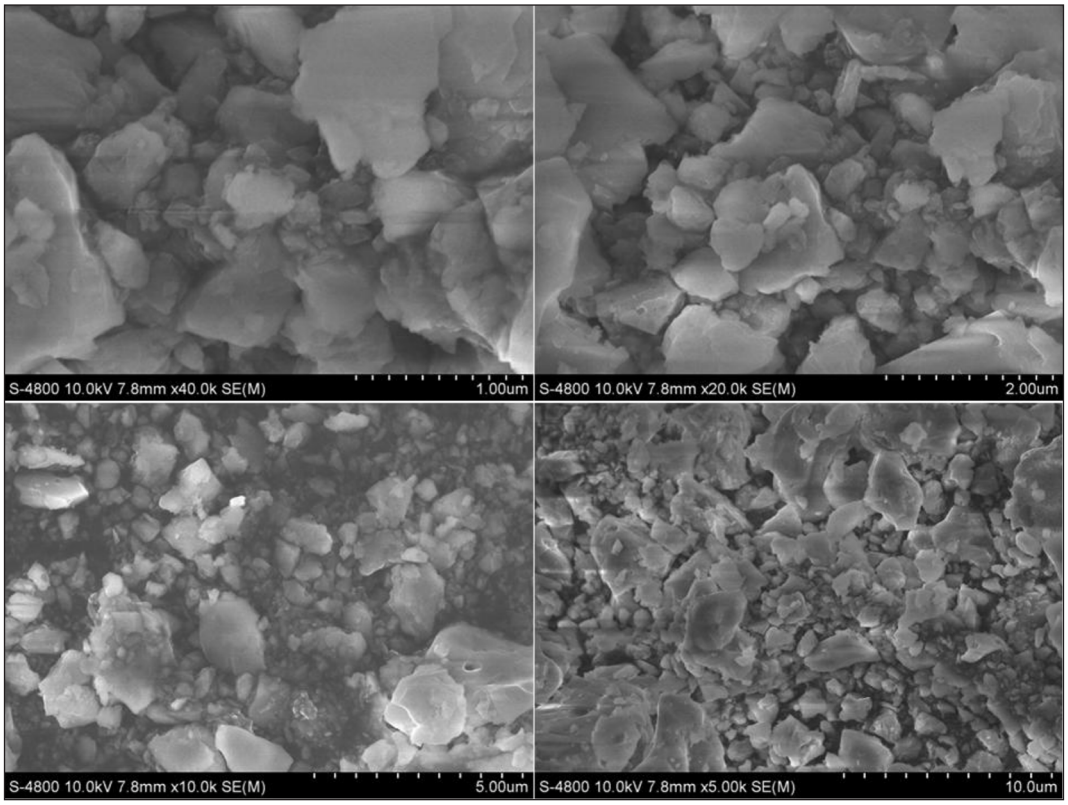


**Figure 3.** The scanning electon microscopy images of calcined clam shells

a denser surface, while the clam shell sample exhibited better particle dispersion, with more clearly defined particle boundaries and the appearance of micro-gaps between particles. However, these differences are primarily morphological and qualitative, and are not sufficient to conclude a significant difference in porosity or pore structure between the two materials. To further clarify the surface characteristics and pore structure observed from SEM images, the $N_2$ adsorption-desorption method based on the BET model was used to determine the specific surface area and pore parameters of the material.

The $N_2$ adsorption-desorption spectra of both oyster shell and clam shell samples after calcination showed a curve shape without a significant increase in the relatively low pressure region ($P/P_0 < 0.1$), and no clear hysteresis loop appeared (Figure 4). This indicates that the material lacks a well-developed pore system, characteristic of materials that are almost non-porous or have very limited pore structure. This isothermal form can be classified close to IUPAC type II or III, commonly found in materials with dense surfaces and weak adsorption interactions. Quantitative results in Table 1 show that the specific surface area ($S_{BET}$) of both samples is very low, reaching 1.049 $m^2/g$ for oyster shells and 0.373 $m^2/g$ for clam shells. This value is much lower than that of typical adsorbent materials (Ali et al. 2025, Tan et al. 2018), indicating that the calcined material did not develop an effective pore system. This is entirely consistent with observations from SEM, where the material surface is strongly aggregated and lacks interconnected capillary structures.

The surface area according to the Langmuir model ($S_{lang}$) also showed low values (1.560 $m^2/g$ for oyster shells and 0.477 $m^2/g$ for clam shells), further confirming the limited adsorption capacity of the material. Notably, the external surface area ($S_{ext}$) accounts for a large proportion of the total surface area ($S_{BET}$), especially in the oyster shell sample (1.120/1.049 $m^2/g$), indicating that the material has almost no micropores, but mainly consists of the external surface of aggregated particles. The total pore volume ($V_{total}$) of both samples was very small (around 0.001–0.0012 $cm^3/g$), and the micropore volume ($V_{micro}$) was almost zero (0–0.0003 $cm^3/g$), indicating that the material lacked a significant micropore system. This is consistent with FTIR results, where the calcination process converted $CaCO_3$ to CaO and caused the collapse of the original pore structure. The release of $CO_2$ during decomposition did not

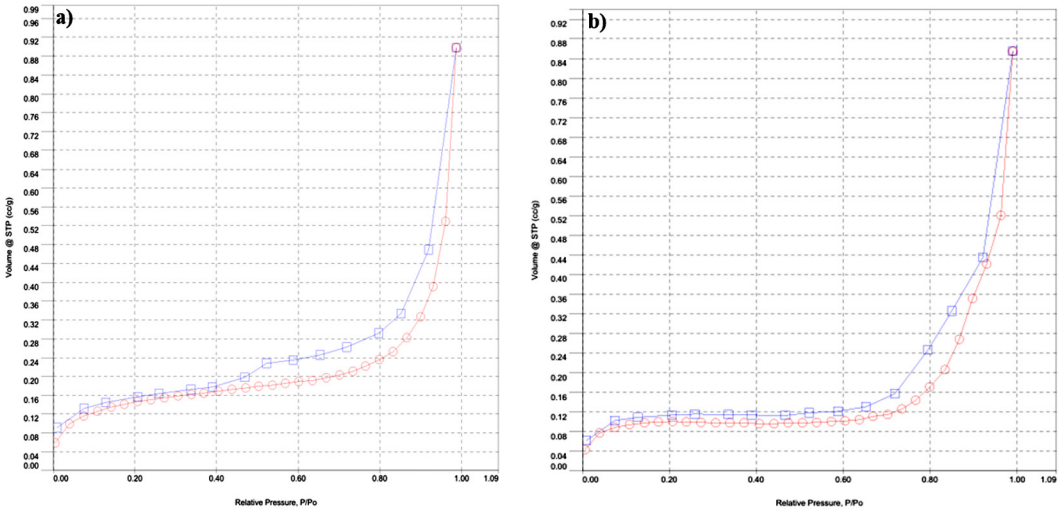


**Figure 4.** BET adsorption-desorption isotherm of calcined oyster shells (a), clam shells (b) (red line – Ads, green line – Des)

create a stable pore system, but instead led to the aggregation and recrystallization of the particles. The average pore diameter ($D_{pore}$) showed a notable difference between the two samples: oyster shells had a value of approximately 12.18 nm, located in the mesopore region, while clam shells were only about 1.04 nm, near the boundary between micropores and mesopores. However, due to the very low pore volume, these values are only representative of local geometry and do not reflect the existence of a well-developed pore system. In other words, although the pore sizes vary, the number of pores is so small that they do not contribute significantly to the surface area. The correlation coefficient (r) of the BET curve is high (0.9998 for oyster shells and 0.99426 for clam shells), indicating that the BET model fits well with the experimental data. The BET constant (C) differs significantly between the two samples (51.24 vs. 214.335), reflecting differences in the degree of interaction between the $N_2$ molecule and the material surface. The high C value in the clam shell sample indicates stronger adsorption interaction, possibly related to differences in surface structure or the degree of CaO phase distribution. The BET results showed that both calcined materials had low surface area, small pore volume, and virtually no micropores, indicating that the porous structure did not develop. The differences between the two samples were mainly in pore size and the degree of adsorption interaction, but not enough to create a significant difference in overall pore characteristics. These results are entirely consistent with SEM (strong aggregation, few pores) and FTIR ($CaCO_3$ into CaO phase transition) observations, suggesting that the calcination process caused the collapse of the pore structure and the formation of a dense surface material.

## Metal ion removal

The results in Figure 5 and Table 2 show that the removal efficiency and adsorption capacity (Qe, mg/g) of $Pb^{2+}$, $Cd^{2+}$, and $Cu^{2+}$ ions on both materials increased significantly as the initial concentration increased from 50 to 150 mg/L. Specifically, for $Pb^{2+}$ on oyster shells, the efficiency increased from 76.84% to 91.53%, while Qe increased sharply from 2.31 to 8.24 mg/g. A similar trend was also observed on clam shells with efficiency reaching 92.14% and Qe reaching 8.29 mg/g at 150 mg/L. For $Cd^{2+}$, the efficiency increased from approximately 63.84–68.55% to 87.06–87.39%, with Qe reaching approximately 7.8 mg/g. While $Cu^{2+}$ exhibited lower efficiency, increasing from approximately 59.63–65.54% to 84.47–85.77%, with a Qe of around 7.6–7.7 mg/g at high concentrations. This increase reflects the crucial role of concentration gradient, as higher concentrations create stronger diffusion dynamics, increasing the probability of collisions between metal ions and the material surface, thereby enhancing removal capacity.

Considering the nature of the metal ions, both materials exhibit a removal tendency in the order $Pb^{2+} > Cd^{2+} > Cu^{2+}$. This trend is consistent with previous findings (Xu et al., 2019). This difference can be explained based on the

**Table 1.** Surface area and porosity of calcined oyster shells and clam shells

| Parameters/Unit | Value | Oyster shells | Clam shells |
|---|---|---|---|
| Specific surface area ($S_{BET}$)/m²/g | Multi-Point BET | 1.049 | 0.373 |
| Langmuir surface area ($S_{lang}$)/m²/g | Langmuir | 1.560 | 0.477 |
| External surface area ($S_{ext}$)/m²/g | V-t Method | 1.120 | 0.216 |
| Total pore volume ($V_{total}$)/cm³/g | at $P/P_0$ = 0.99 | 0.0012 | 0.001 |
| Micropore volume ($V_{micro}$)/cm³/g | DA Method | 0.0003 | 0.000 |
| Average pore diameter ($D_{pore}$)/nm | BJH Adsorption | 12.18 | 1.0417 |
| Correlation coefficient ($r$) | BET Plot | 0.9998 | 0.99426 |
| BET constant ($C$) | BET Plot | 51.24 | 214.335 |

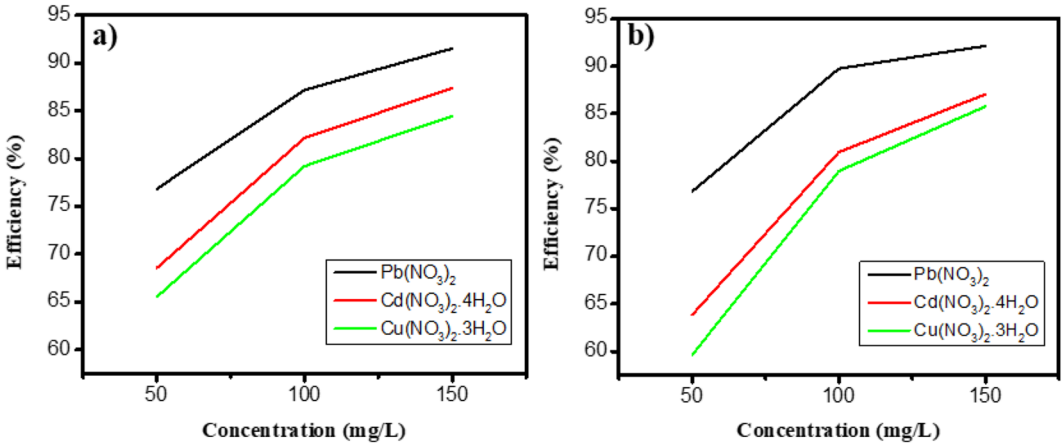


**Figure 5.** Removal efficiency of $Pb^{2+}$, $Cd^{2+}$, and $Cu^{2+}$ ions by calcined oyster shells (a) and clam shells (b)

physicochemical factors of the ions, including ionic radius, hydration energy, and precipitation ability in alkaline environments. $Pb^{2+}$ has a larger radius and lower hydration energy compared to $Cd^{2+}$ and $Cu^{2+}$, making it more susceptible to detachment from the hydration shell and interaction with the CaO surface. At the same time, in the alkaline environment created by CaO, $Pb^{2+}$ readily forms less soluble precipitates such as $Pb(OH)_2$ or $PbCO_3$, increasing removal efficiency. Meanwhile, $Cu^{2+}$ tends to form stable complexes in solution and has a higher hydration energy, resulting in lower removal efficiency. A comparison between the two materials shows that the performance differences are relatively small and not clearly systematic. For example, for $Pb^{2+}$ at 150 mg/L, clam shells showed slightly higher efficiency (92.14% vs. 91.53%), while for $Cd^{2+}$ and $Cu^{2+}$, the difference between the two materials only ranged from 1–3%. This suggests that the chemical nature of the calcined materials is similar, with the main active phase being CaO, and the treatment efficiency is primarily governed by the chemical mechanism rather than the physical structure. Notably, although the BET results showed a very low specific surface area of the material (≤ 1.049 m²/g) and SEM showed an agglomerated structure with poorly developed pores, the metal removal efficiency still reached high values. This demonstrates that the removal mechanism is not governed by physical adsorption on the surface, but mainly involves chemical processes such as metal precipitation in alkaline environments (due to CaO hydrolysis to form $Ca(OH)_2$), ion exchange between $Ca^{2+}$ and heavy metal ions, as well as secondary surface adsorption. Thus, the heavy metal removal efficiency of the material does not depend much on the surface area but mainly on the chemical properties and alkalinity of the material after calcination.

Based on FT-IR, SEM, and BET results, although the calcined material has a low surface area and poorly developed porous structure, the removal efficiency of $Pb^{2+}$, $Cd^{2+}$, and $Cu^{2+}$ is still high, indicating that the treatment mechanism is

**Table 2.** Comparison of removal efficiency (H, %) and adsorption capacity (Qe, mg/g) for $Pb^{2+}$, $Cd^{2+}$, and $Cu^{2+}$ on calcined oyster and clam shells at different initial concentration

| Parameter | Ions | Conc (mg/L) | H (%) | Qe (mg/g) |
|---|---|---|---|---|
| Calcined oyster shells | $Pb(NO_3)_2$ | 50 | 76.84 | 2.31 |
| | | 100 | 87.18 | 5.23 |
| | | 150 | 91.53 | 8.24 |
| | $Cd(NO_3)_2.4H_2O$ | 50 | 68.55 | 2.06 |
| | | 100 | 82.16 | 4.93 |
| | | 150 | 87.39 | 7.87 |
| | $Cu(NO_3)_2.3H_2O$ | 50 | 65.54 | 1.97 |
| | | 100 | 79.21 | 4.75 |
| | | 150 | 84.47 | 7.60 |
| Calcined clam shells | $Pb(NO_3)_2$ | 50 | 76.83 | 2.31 |
| | | 100 | 89.75 | 5.38 |
| | | 150 | 92.14 | 8.29 |
| | $Cd(NO_3)_2.4H_2O$ | 50 | 63.84 | 1.92 |
| | | 100 | 80.96 | 4.86 |
| | | 150 | 87.06 | 7.84 |
| | $Cu(NO_3)_2.3H_2O$ | 50 | 59.63 | 1.79 |
| | | 100 | 78.97 | 4.74 |
| | | 150 | 85.77 | 7.72 |

not dominated by purely physical adsorption but mainly involves chemical processes. When in contact with water, the CaO in the material is rapidly hydrated to form $Ca(OH)_2$ according to the reaction (3):

$$CaO + H_2O \rightarrow Ca(OH)_2 \quad (3)$$

This process increases the pH of the solution, creating a strongly alkaline environment, thereby promoting the precipitation of metal ions in the form of insoluble hydroxides (4):

$$M^{2+} + 2OH^- \rightarrow M(OH)_2 \downarrow (M = Pb, Cd, Cu) \quad (4)$$

In which, $Pb^{2+}$ tends to precipitate more strongly due to its solubility $Pb(OH)_2$ is lower than $Cd(OH)_2$ and $Cu(OH)_2$, resulting in higher removal efficiency, consistent with the order $Pb^{2+} > Cd^{2+} > Cu^{2+}$ observed in the experiment. In addition, since the material still contains some $CaCO_3$ after calcination (according to FTIR results), metal ions can also participate in the carbonate precipitation reaction (5):

$$M^{2+} + 2CO_3^{2-} \rightarrow MCO_3 \downarrow \quad (5)$$

A small fraction of metal ions can be retained on the material surface through surface adsorption; however, due to the low surface area, this mechanism does not play a dominant role. Thus, the heavy metal removal mechanism of the material is mainly a combination of hydroxide precipitation in alkaline environments, carbonate precipitation, and ion exchange, with chemical precipitation being the primary mechanism determining treatment efficiency.

## CONCLUSIONS

This research has demonstrated that calcined oyster and clam shells can be used as low-cost materials for the efficient removal of $Pb^{2+}$, $Cd^{2+}$, and $Cu^{2+}$ from water. FTIR, SEM, and BET results show that the material has an agglomerated structure, low surface area, and poorly developed capillaries. However, the removal efficiency remains high, especially for $Pb^{2+}$ (>90% at 150 mg/L), with a trend of $Pb^{2+} > Cd^{2+} > Cu^{2+}$. This indicates that the treatment mechanism does not depend on physical adsorption but is mainly due to chemical processes, including CaO hydration to create an alkaline environment, precipitation of hydroxides and carbonates, and ion exchange. The results confirm that calcined shell materials are an effective, sustainable, and promising solution for treating water contaminated with heavy metals.

## Acknowledgement

The authors acknowledge the support from Thu Dau Mot University and thank all individuals who contributed to this research.

## REFERENCES

1. Ali, H., Khan, E., Ilahi, I. (2019). Environmental chemistry and ecotoxicology of hazardous heavy metals: Environmental persistence, toxicity, and bioaccumulation. *Journal of Chemistry*, *2019*, 6730305. https://doi.org/10.1155/2019/6730305
2. Ali, M. B., Bakhtaoui, Y., Flayou, M., El Hazzat, M., Sifou, A., Dahhou, M., Kacimi, M., Benzaouak, A., El Hamidi, A. (2025). Adsorption of brilliant cresyl blue using NaOH-activated biochar derived from sewage sludge. In: *E3S Web of Conferences*, *601*, 00087.https://doi.org/10.1051/e3sconf/202560100087
3. Balali-Mood, M., Naseri, K., Tahergorabi, Z., Khazdair, M. R., Sadeghi, M. (2021). Toxic mechanisms of five heavy metals: Mercury, lead, chromium, cadmium, and arsenic. *Frontiers in Pharmacology*, *12*, 643972. https://doi.org/10.3389/fphar.2021.643972
4. Lin, P.Y., Wu, H.M., Hsieh, S.L., Li, J.S., Dong, C., Chen, C.W., Hsieh, S. (2020). Preparation of vaterite calcium carbonate granules from discarded oyster shells as an adsorbent for heavy metal ions removal. *Chemosphere, 254*, 126903. https://doi.org/10.1016/j.chemosphere.2020.126903
5. Núñez, D., Serrano, J. A., Mancisidor, A., Elgueta, E., Varaprasad, K., Oyarzún, P., Cáceres, R., Ide, W., & Rivas, B. L. (2019). Heavy metal removal from aqueous systems using hydroxyapatite nanocrystals derived from clam shells. *RSC Advances, 9*, 22883–22890. https://doi.org/10.1039/C9RA04198B
6. Oladimeji, T., Oyedemi, M., Emetere, M., Agboola, O., Adeoye, J., Odunlami, O. (2024). Review on the impact of heavy metals from industrial wastewater effluent and removal technologies. *Heliyon*, 10,e40370. https://doi.org/10.1016/j.heliyon.2024.e40370
7. Rashid, R., Shafiq, I., Akhter, P., Iqbal, M. J., Hussain, M. (2021). A state-of-the-art review on wastewater treatment techniques: The effectiveness of adsorption method. *Environmental Science and Pollution Research, 28*, 9050–9066. https://doi.org/10.1007/s11356-021-12395-x
8. Rosli, S., Jameel, M., Mayzan, M., Shamsuddin, S., M-Raffi, M., Zainal, A., Saleem, S. (2024). Simple thermal treatment of waste oyster (*Crassostrea belcheri*) shells for the production of calcium minerals in biomaterials application. *Nature Biotechnology Engineering*. https://doi.org/10.26599/NBE.2024.9290074
9. Sun, C., Qiu, J., Zhang, Z., Marhaba, T. F., Zhang, Y., Zhang, W. (2016). Characterization of citric acid-modified clam shells and application for aqueous lead (II) removal. *Water, Air, & Soil Pollution*, 227, 298. https://doi.org/10.1007/s11270-016-2998-2
10. Wang, H., Fu, Y., Guo, K., Li, X., Jin, X., Huang, Y., Wang, X., Lu, G., Yi, X., Dang, Z. (2024). Novel magnetic adsorbents based on oyster and clam shells for the removal of cadmium in soil. *Science of the Total Environment, 955*, 177083. https://doi.org/10.1016/j.scitotenv.2024.177083
11. Xia, C., Zhang, X., Xia, L. (2021). Heavy metal ion adsorption by permeable oyster shell bricks. *Construction and Building Materials*, 275, 122128. https://doi.org/10.1016/j.conbuildmat.2020.122128
12. Xu, X., Liu, X., Oh, M., Park, J. (2019). Oyster shell as a low-cost adsorbent for removing heavy metal ions from wastewater. *Polish Journal of Environmental Studies*, *28*, 2949–2959. https://doi.org/10.15244/pjoes/92941
13. Xu, Z., Valeo, C., Chu, A., Zhao, Y. (2021). The efficacy of whole oyster shells for removing copper, zinc, chromium, and cadmium heavy metal ions from stormwater. *Water*, *13*, 4184. https://doi.org/10.3390/su13084184
14. Tan, Z., Zou, J., Zhang, L., Huang, Q. (2018). Morphology, pore size distribution, and nutrient characteristics in biochars under different pyrolysis temperatures and atmospheres. *Journal of Material Cycles and Waste Management*, *20*, 1036–1049. https://doi.org/10.1007/s10163-017-0666-5